催化学报
2011 Chinese Journal of Catalysis Vol. 32 No. 2

文章编号: 0253-9837(2011)02-0217-07 国际版 DOI: 10.1016/S1872-2067(10)60167-2 研究快讯: 217~223

动态水热合成*b*轴取向MFI型分子筛膜

李显明[1], 王正宝[1], 郑 洁[1], 邵世群[1], 王胤超[1], 严玉山[1,2]

[1]浙江大学化学工程与生物工程学系, 浙江杭州 310027

[2]加州大学河滨分校化学工程与环境工程系, 美国加利福尼亚州 92521

摘要: 在旋转烘箱中采用动态水热法,在不锈钢片支撑体上合成了连续的*b*轴取向MFI型分子筛膜,并运用扫描电镜和X射线衍射考察了合成釜转速、晶化温度和晶化时间对所得分子筛膜性能的影响. 与静态水热法相比,动态水热合成过程中合成液的温差和浓度差大大降低,且合成液持续冲刷支撑体表面,使得动态法具有合成时间短、取向性好和分子筛颗粒粒径分布均一的优点.

关键词: 动态水热法; *b*轴取向; MFI型分子筛; 分子筛膜; 静态水热法

中图分类号: O643 **文献标识码:** A

Dynamic Hydrothermal Synthesis of a *b*-Oriented MFI Zeolite Film

LI Xianming[1], WANG Zhengbao[1,*], ZHENG Jie[1], SHAO Shiqun[1], WANG Yinchao[1], YAN Yushan[1,2]

[1]*Department of Chemical and Biochemical Engineering, Zhejiang University, Hangzhou 310027, Zhejiang, China*

[2]*Department of Chemical and Environmental Engineering, University of California, Riverside, California 92521, USA*

Abstract: Continuous *b*-oriented MFI zeolite films were prepared on stainless steel substrates by dynamic hydrothermal synthesis using a rotating convection oven. The influences of rotation speed, crystallization temperature and crystallization time were studied. X-ray diffraction was used to identify the orientation of the zeolite films. Compared with the static method, a shorter synthesis time, a more uniform particle size distribution and better film orientation were observed for the dynamic method, and this is attributed to the low concentration and thermal gradients that exist in the bulk solution and to the washing action of the bulk solution toward the substrate surface.

Key words: dynamic hydrothermal method; *b*-oriented; MFI zeolite; zeolite film; static hydrothermal method

近几十年来,分子筛膜因具有均一的孔径、特定的催化性能、低介电常数、良好的热稳定性和化学稳定性而广泛应用于物质分离[1~5]、膜反应器[6,7]、电子材料[8~10]和防腐材料[11,12]等领域. 在MFI分子筛晶体内, *b*轴取向0.53 nm × 0.56 nm的直孔道与*a*轴取向0.51 nm × 0.55 nm的正弦孔道相交叉,由于*b*轴取向分子筛膜直孔道垂直于支撑体表面,因而具有更广泛的应用前景. 晶种法(二次生长法)是合成取向性分子筛膜的常见方法[1,13~15],晶种层的应用有利于精确控制分子筛膜的二次生长,但是其涂覆较为复杂. Wang等[16,17]在不锈钢支撑体上原位合成了*b*轴取向MFI型分子筛膜,方法简单,节能且成本较低.

现在绝大多数分子筛膜均采用静态水热法合成. 在合成过程中,分子筛膜与合成液界面处的营养被迅速消耗,在体相溶液中形成较大的浓度差,并且可能会改变溶液组成. 此外,由于缺乏有效的热交换,体相溶液中常常存在较大的温差. 而较大的浓度差和温差将导致膜层缺陷,影响分子筛膜的性能. 此外,静态合成时的重力沉降作用也不利于形成均匀的膜层. 为了减少或避免上述不利因素的影响,人们尝试在动态环境下合成分子筛膜[18~24]. Yamazaki

收稿日期: 2010-10-08. **接收日期:** 2010-11-22.

联系人: 王正宝. Tel/Fax: (0571)87952391; E-mail: zbwang@zju.edu.cn

基金来源: 浙江省自然科学基金(R4090099); 中国博士后科学基金(20090461362, 201003718); 南京工业大学材料化学工程国家重点实验室开放课题.

本文的英文电子版由Elsevier出版社在ScienceDirect上出版(http://www.sciencedirect.com/science/journal/18722067).

等[22]在循环溶液系统中合成高纯度 A 型分子筛, 而静态合成时产生了部分副产物. Tiscareño-Lechuga 等[23]在管状支撑体的内腔合成分子筛膜, 合成装置高速旋转产生的离心力有助于形成连续的致密膜. Huang 等[24]采用真空辅助方法在 α-Al_2O_3 管上合成了均匀致密的 NaA 分子筛膜, 该方法有效减少了重力的负面作用. 本文采用一种新的使合成釜旋转的动态合成装置来制备 *b* 轴取向 MFI 型分子筛膜.

不锈钢支撑体上的纯硅 MFI (silicalite-1) 型分子筛膜的制备如下: 将镜面 202 不锈钢片 (20 mm × 20 mm) 支撑体在双氧水中浸泡 45 min 后, 用去离子水清洗、在 60 °C 干燥. 搅拌下将正硅酸乙酯 (TEOS, Acros Organics) 加入到四丙基氢氧化铵 (TPAOH, 浙江省仙居县医药化工实验厂) 水溶液中, 合成液摩尔组成为 1TEOS:0.32TPAOH:165H_2O, 室温搅拌 4 h 后得澄清透明溶液, 然后将此溶液 (90 g) 和支撑体一起放到带有聚四氟乙烯内衬的 110 ml 合成釜内, 密封后放入旋转烘箱中晶化. 动态合成装置的结构如图 1 所示, 支撑体用聚四氟乙烯支架固定后竖直浸没于合成液中, 合成釜固定在烘箱转动轴的支架上随轴转动. 晶化后, 将支撑体取出, 用去离子水浸泡, 清洗, 并在 60 °C 干燥.

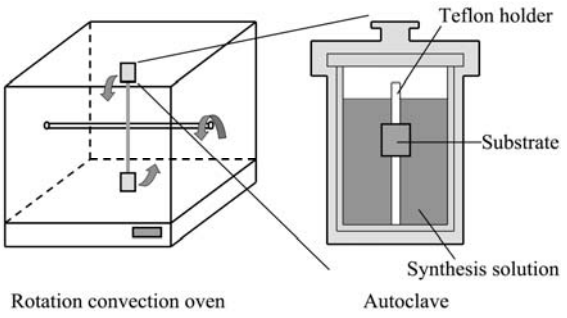

图 1 合成分子筛膜的动态合成装置

Fig. 1. The experimental apparatus used in this work to synthesize zeolite films.

分子筛膜的表面形貌在 Hitachi S-4800 型扫描电镜 (SEM) 上观察. 分子筛的 X 射线衍射 (XRD) 谱由 Panalytical X' PertPro 型 X 射线衍射仪测得.

为了研究静态和动态水热合成分子筛膜的差别, 本文首先研究了合成釜转速 (*R*) 对合成分子筛膜的影响, 所得样品的 SEM 照片如图 2 所示. 可以看出, 所有 MFI 型分子筛膜均以 *b* 轴取向为主. 在较低

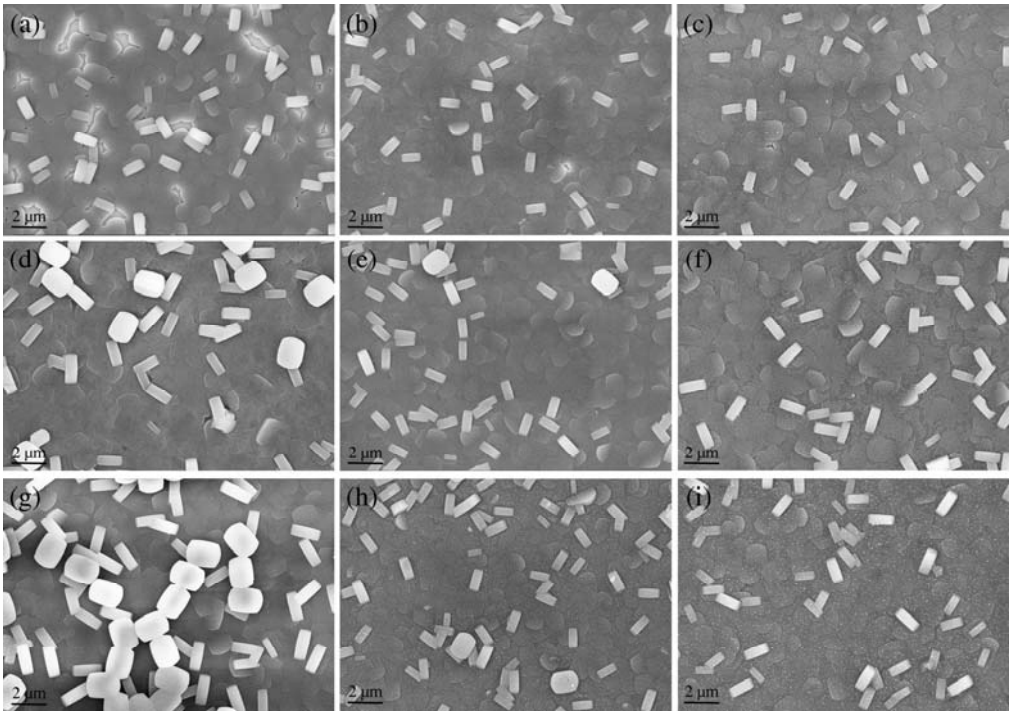

图 2 不同温度不同转速下合成 2 h 分子筛膜的 SEM 照片

Fig. 2. SEM micrographs of the MFI zeolite films on stainless steel substrates synthesized at various temperatures for 2 h at different rotation speeds. (a) 165 °C, 0 r/min; (b) 165 °C, 10 r/min; (c) 165 °C, 20 r/min; (d) 170 °C, 0 r/min; (e) 170 °C, 10 r/min; (f) 170 °C, 20 r/min; (g) 175 °C, 0 r/min; (h) 175 °C, 10 r/min; (i) 175 °C, 20 r/min.

温度 (165 ºC) 下静态 (R = 0 r/min) 合成的分子筛膜中存在大量缺陷, 且有 *a* 轴取向晶体存在 (图 2(a)). 当合成釜转速增加到 10 和 20 r/min 时, 动态合成得到只有少量针孔的分子筛膜 (图 2(b) 和 (c)). 与静态合成相比, 动态合成显著降低了膜层中的缺陷数量. 165 ºC 时所得分子筛晶体的尺寸均为 0.9 μm.

升高温度有利于分子筛的生长, 如图 2(d) 所示, 当晶化温度升至 170 ºC 时, 晶粒尺寸增大到 1.1 μm, 静态合成得到了近似连续的分子筛膜, 但存在较多的第二层分子筛. 值得注意的是, 当合成釜转速增加到 10 和 20 r/min 时, 动态合成得到了连续的分子筛膜 (图 2(e) 和 (f)), 并且第二层分子筛晶体的数量较少, 膜层较光滑.

进一步升高晶化温度至 175 ºC, 晶粒尺寸增加到 1.2 μm. 静态合成得到了连续的分子筛膜 (图 2(g)), 但产生了很多第二层分子筛. 动态合成也能得到连续的分子筛膜层, 且较光滑 (图 2(h) 和 (i)). 这表明合成釜的转动能减少致密膜上第二层分子筛的形成.

在我们之前的报道中, 165 ºC 静态合成 2 h 可得到连续的分子筛膜[16,17,25], 而在本文中则不能, 其原因主要是合成液用量不同所致. 前者合成液用量 (20 g) 不到合成釜容积的 1/3, 而本文却超过了 2/3, 因此本文中合成液需更长时间以升至指定温度.

XRD 表征可确认分子筛膜的取向性, 图 3 给出了所得样品 XRD 谱. 可以看出, 除了不锈钢支撑体所对应的 2θ = 43.46º 峰以外, MFI 型分子筛膜在 2θ = 8.87º, 17.77º, 26.80º, 35.99º 和 45.45º 处有 5 个尖峰, 分别对应于 (020), (040), (060), (080) 和 (0100) 晶面[26], 即所制 MFI 型分子筛膜为 *b* 轴取向. 但在静态法合成样品上于 2θ = 35.75º 和 45.15º 处有两个小峰, 分别对应于 (800) 和 (1000) 晶面[26]. 这表明静态法所得分子筛膜中有部分 *a* 轴取向的晶体存在. 将其谱图放大才能观察到 (200), (400) 和 (600) 晶面衍射峰, 强度很低, 且与 (020), (040) 和 (060) 晶面衍射峰部分重叠, 因而难以分辨. 比较而言, 动态法样品上 (800) 和 (1000) 晶面衍射峰要小很多, 即所得分子筛膜中 *a* 轴取向分子筛较少. 上述结果表明动态水热法所得分子筛膜的取向性更好.

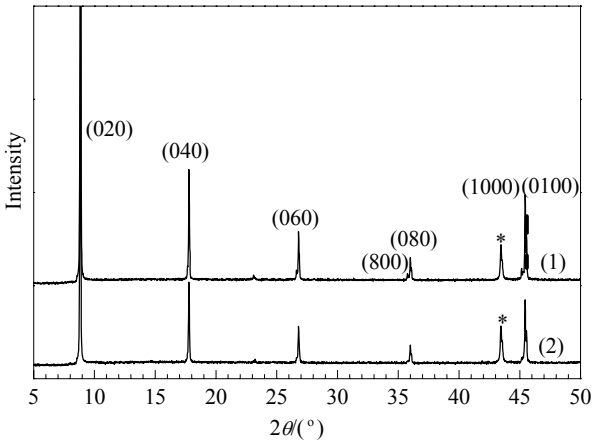

图 3 静态和动态方法 170 ºC 合成 2 h 所得分子筛膜的 XRD 谱

Fig. 3. XRD patterns of the zeolite films synthesized at 170 ºC for 2 h. (1) The static method (0 r/min); (2) The dynamic method (20 r/min).

静态和动态水热法的合成条件不同, 所得分子筛晶粒的粒径分布也将不同. 图 4 为不同转速下体相溶液中分子筛颗粒的 SEM 照片. 可以看出, 静态合成所得分子筛颗粒的粒径分布不均, 其大小为 0.6 到 1.1 μm. 而动态合成所得分子筛颗粒的粒径分布较为均一 (图 4(b) 和 (c)). 粒径分布的差异应当与合成釜的转动有关. 在静态环境下, 重力沉降作用和晶粒周围营养的迅速消耗造成了较大的浓度差. 另外, 由于缺少有效的搅拌, 静态环境还存在较大的温差. 而在动态环境下, 合成釜的旋转使得合成液能够进行有效的传热传质, 因此体相溶液中温差和浓度差

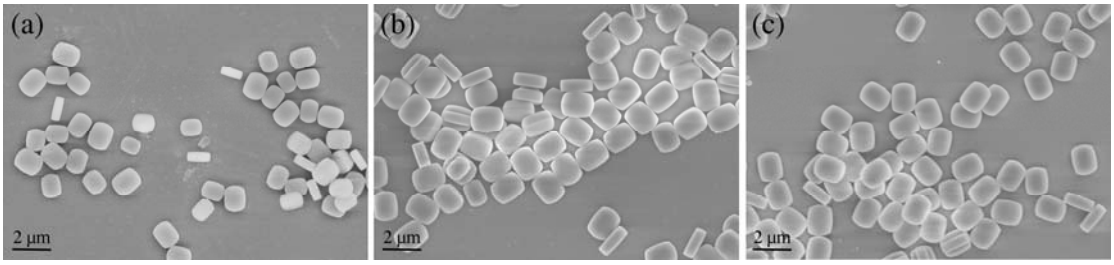

图 4 不同转速下 170 ºC 合成 2 h 所得体相溶液中分子筛颗粒的 SEM 照片

Fig. 4. SEM micrographs of MFI zeolite crystals in the bulk solution synthesized at 170 ºC for 2 h at different rotation speeds. (a) 0 r/min; (b) 10 r/min; (c) 20 r/min.

很小, 有利于得到粒径均一的分子筛颗粒.

为了研究分子筛膜的生长过程, 本文还考察了170 ºC下晶化时间对合成分子筛膜的影响, 所得样品的SEM照片见图5. 可以看出, 对于静态法, 晶化80 min时支撑体上仍未观察到分子筛(图5(a)), 90 min时支撑体上有少量圆盘状晶体存在. 进一步晶化至100和110 min (图5(c)和(d)), 圆盘状晶体长大并相互连接. 至120 min (图2(d))时得到了有部分针孔的近似连续膜, 且可观察到有第二层分子筛颗粒. 继续晶化至140 min时才能得到连续的分子筛膜.

对于动态法, 在晶化早期(80 min)形成了一些亚微米级(0.3 μm)的圆盘状晶体(图5(e)). 90 min时, 晶体长大到0.5 μm (图5(f)), 并且相互连接. 晶化至100和110 min, 晶体进一步长大到0.6和0.9 μm (图5(g)(h)), 形成了近似连续的分子筛膜. 至120 min时, 晶粒长大到1.1 μm, 得到连续的分子筛膜(图2(f)).

静态和动态法所合成分子筛膜的差异是由合成釜的转动造成的. 由于支撑体被固定在合成釜的中间, 并且静态法存在较大的温差, 因此支撑体附近的合成液需要较长的时间才能升至指定温度, 这使得在相同晶化时间静态法的支撑体上分子筛颗粒数量比动态法的少.

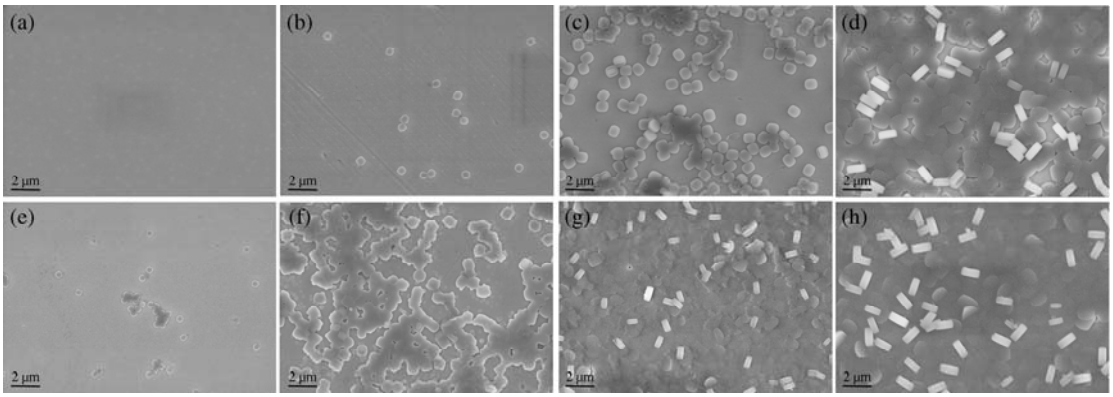

图 5 静态和动态法合成不同时间所得分子筛膜的 SEM 照片

Fig. 5. SEM micrographs of MFI zeolite films on stainless steel substrates synthesized at 170 ºC for different time using the static (a~d, R = 0 r/min) and dynamic (e~h, R = 20 r/min) methods. (a,e) 80 min; (b,f) 90 min; (c,g) 100 min; (d,h) 110 min.

结合我们之前提出的均相成核机理[16,17,27]和上述实验结果, 本文认为动态合成分子筛膜的成膜机理如下: 合成液在室温搅拌过程中形成了部分晶核; 更多的晶核在晶化初期(体相溶液的温度远低于设定的晶化温度)形成, 并且长大成亚微米级(0.3 μm)的晶体, 部分亚微米级晶体由于范德华力和静电引力的作用被吸附到支撑体表面; 随着晶化的继续, 更多的晶体被吸附到支撑体表面并长大; 进一步晶化, 支撑体上的晶体交联生长并形成连续的分子筛膜. 对于动态法, 体相溶液中浓度差和温差都很小, 合成液升温较快, 因此合成连续膜所需时间较短.

由于MFI型分子筛晶体(010)面的面积最大, 因此亚微米级晶体吸附到支撑体表面的最稳定结构就是*b*轴取向, *b*轴取向晶体与支撑体表面的作用强于*a*轴取向晶体与支撑体表面的作用. 静态法所合成的分子筛膜中仍有部分*a*轴取向的晶体存在. 而在动态环境下, 由于体相溶液对支撑体表面的冲刷作用, 多数被吸附到支撑体表面的*a*轴取向晶体被冲刷掉或者倒向支撑体表面(变成*b*轴取向), 从而有利于合成取向性更好、表面更光滑的分子筛膜. 此外, 由于冲刷作用而倒下的*a*轴取向晶体也可能填补缺陷位, 从而有利于合成连续膜.

综上所述, 本文采用旋转烘箱, 动态水热合成了*b*轴取向MFI型分子筛膜. 与静态方法相比, 动态水热合成有如下优点: (1) 合成连续膜耗时短; (2) MFI型分子筛膜的取向性更好、表面更光滑; (3) 晶粒尺寸分布均一.

参 考 文 献

1 Lai Z P, Bonilla G, Diaz I, Nery J G, Sujaoti K, Amat M A, Kokkoli E, Terasaki O, Thompson R W, Tsapatsis M, Vlachos D G. *Science*, 2003, **300**: 456
2 Chen H L, Li Y S, Yang W S. *J Membr Sci*, 2007, **296**: 122
3 Zhao Q Y, Wang J Q, Chu N B, Yin X Y, Yang J H, Kong C L, Wang A F, Lu J M. *J Membr Sci*, 2008, **320**: 303
4 陈红亮, 李砚硕, 刘杰, 杨维慎, 林励吾. 催化学报 (Chen H

L, Li Y Sh, Liu J, Yang W Sh. *Chin J Catal*), 2005, **26**:1039
5 周汉, 李砚硕, 朱广奇, 刘杰, 林励吾, 杨维慎. 催化学报 (Zhou H, Li Y Sh, Zhu G Q, Liu J, Lin L W, Yang W Sh. *Chin J Catal*), 2008, **29**: 592
6 Yeung K L, Zhang X F, Lau W N, Martin-Aranda R. *Catal Today*, 2005, **110**: 26
7 Wang X D, Zhang B Q, Liu X F, Lin J Y S. *Adv Mater*, 2006, **18**: 3261
8 Liu Y, Lew C M, Sun M W, Cai R, Wang J L, Kloster G, Boyanov B, Yan Y S. *Angew Chem*, *Int Ed*, 2009, **48**: 4777
9 Wang Z B, Mitra A P, Wang H T, Huang L M, Yan Y S. *Adv Mater*, 2001, **13**: 1463
10 Wang Z B, Wang H T, Mitra A, Huang L M, Yan Y S. *Adv Mater*, 2001, **13**: 746
11 Cai R, Sun M W, Chen Z W, Munoz R, O'Neill C, Beving D E, Yan Y S. *Angew Chem*, *Int Ed*, 2008, **47**: 525
12 Beving D E, McDonnell A M P, Yang W S, Yan Y S. *J Electrochem Soc*, 2006, **153**: B325
13 Wee L H, Wang Z, Tosheva L, Itani L, Valtchev V, Doyle A M. *Microporous Mesoporous Mater*, 2008, **116**: 22
14 Lee I, Buday J L, Jeong H K. *Microporous Mesoporous Mater*, 2009, **122**: 288
15 Liu Y, Li Y S, Yang W S. *J Am Chem Soc*, 2010, **132**: 1768
16 Wang Z B, Yan Y S. *Microporous Mesoporous Mater*, 2001, **48**: 229
17 Wang Z B, Yan Y S. *Chem Mater*, 2001, **13**: 1101
18 Aguado S, Gascon J, Jansen J C, Kapteijn F. *Microporous Mesoporous Mater*, 2009, **120**: 170
19 Khajavi S, Kapteijn F, Jansen J C. *J Membr Sci*, 2007, **299**: 63
20 Pera-Titus M, Mallada R, Llorens J, Cunill F, Santamaria J. *J Membr Sci*, 2006, **278**: 401
21 Xu H H, Shah D B, Talu O. *Zeolites*, 1997, **19**: 114
22 Yamazaki S, Tsutsumi K. *Microporous Mesoporous Mater*, 2000, **37**: 67
23 Tiscareño-Lechuga F, Tellez C, Menendez M, Santamaria J. *J Membr Sci*, 2003, **212**: 135
24 Huang A S, Yang W S, Liu J. *Sep Purif Technol*, 2007, **56**: 158
25 Li X M, Yan Y S, Wang Z B. *Ind Eng Chem Res*, 2010, **49**: 5933
26 Treacy M M J, Higgins J B. Collection of Simulated XRD Powder Patterns for Zeolites. 5th revised Ed. Amsterdam: Elsevier, 2007. 276
27 Li S, Li Z J, Bozhilov K N, Chen Z W, Yan Y S. *J Am Chem Soc*, 2004, **126**: 10732

英 译 文

English Text

Over the last several decades a large amount of effort has been dedicated to the synthesis of zeolite films and membranes because of their unique properties and potential applications. They are used as separation membranes [1–5] because of their uniform pore sizes at the molecular level, membrane reactors [6,7] because of their catalytic performance, electronic materials [8–10] because of their low dielectric constant, and corrosion protection coatings [11,12] because of their high thermal stability and excellent solvent resistance. MFI zeolite films have been widely investigated because of their appropriate pore openings and their three dimensional pore structures. In the MFI zeolite crystal, 0.53 nm × 0.56 nm straight channels (*b*-axis) are interconnected with 0.51 nm × 0.55 nm sinusoidal channels (*a*-axis). Therefore, *b*-oriented MFI films have excellent performance because the straight channels are perpendicular to the substrates, which is interesting from an academic and a practical viewpoint. The seeded growth method is often used to synthesize oriented zeolite films [1,13–15]. The use of oriented seed offers a way to accurately control the growth of a zeolite film. However, the coating of seed results in this method being complex and expensive. Wang et al. [16,17] reported the synthesis of *b*-oriented MFI films on stainless steel substrates using direct in situ crystallization. The advantage of the in situ method is its simplicity, which reduces energy consumption and operation cost.

Most zeolite film syntheses are carried out using the static hydrothermal method. During the film formation process the nutrition are consumed quickly at the interface of the zeolite film and the synthesis solution, which results in a large concentration gradient in the bulk solution and this might change the solution's composition. Moreover, large thermal gradients often exist in the bulk solution as no effective convection occurs during the static hydrothermal process. The high concentration and large thermal gradients might result in defects and this will affect film performance significantly. Furthermore, gravity settling results in a non-uniform zeolite film in an idle state. Some new methods have been investigated under dynamic environments to avoid or reduce the negative influences mentioned above [18–24]. Yamazaki et al. [22] found that only the A-type zeolite formed when using a circulated solution system while the formation of by-products was observed for the static method. Tiscareño-Lechuga et al. [23] reported a new system for the synthesis of zeolite membranes in the lumen of tubular supports. The supports were placed inside a device that rotated around a longitudinal axis during the synthesis. The centrifugal forces produced by the high rotational speed facilitated the formation of a more continuous and dense layer. Huang et al. [24] synthesized uniform and dense NaA zeolite membranes on tubular α-Al_2O_3 supports using a vacuum-assisted method. The negative influence of the gravitational force was effectively reduced in vacuo. In this work, we used a new dynamic synthesis apparatus to produce a *b*-oriented MFI zeolite film in which the synthesis conditions were dynamic because of rotation of the autoclave.

Pure silica MFI (silicalite-1) films on stainless steel substrates were prepared as follows: Mirror stainless steel 202

plates (20 nm × 20 mm) were immersed in a hydrogen peroxide solution for 45 min and then rinsed with deionized water after which it was dried at 60 °C before the synthesis of the zeolite films.

A synthesis solution with a molar composition of 1TEOS:0.32TPAOH:165H_2O was made by slowly adding tetraethylorthosilicate (TEOS, Acros Organics) to a solution of tetrapropylammonium hydroxide (TPAOH, Zhejiang Xianju Application Chemical Research Institute, China) and water while stirring. A clear synthesis solution was obtained after stirring at room temperature for 4 h. The synthesis solution (90 g) was loaded directly without filtering into a Teflon-lined stainless steel autoclave (110 ml). Figure 1 shows the experimental apparatus used in this work to synthesize the zeolite films. A metal substrate was placed vertically in a Teflon holder at the middle of the autoclave and immersed into the synthesis solution. The autoclave was then sealed and heated in a rotating convection oven at a specific temperature and held there for a certain amount of time. In the rotating convection oven the autoclaves were fixed in a stationary barrier, which could rotate with the axis. After the synthesis the mixture was quenched. The samples were recovered, thoroughly washed with deionized water, and dried at 60 °C.

The morphology of the silicalite films synthesized was examined by scanning electron microscopy (SEM) at 8 kV using a Hitachi S-4800 microscope. X-ray diffraction (XRD) patterns were collected on a Panalytical X' PertPro diffractometer using Cu K_α radiation.

To investigate the differences in zeolite film formation between the static and dynamic hydrothermal synthesis the rotation speed (R) of the autoclave was varied from 0 to 20 r/min (Fig. 2). All the MFI zeolite films were predominantly *b*-oriented. As shown in Fig. 2(a), at the low crystallization temperature of 165 °C, a discontinuous film with many defects was obtained for the static method (R = 0 r/min). Some *a*-oriented crystals were also present. When the autoclave was stirred at 10 and 20 r/min a nearly continuous film with a few pinholes was obtained (Fig. 2(b) and (c)). Compared with the film synthesized by the static method, the amount of defects in the zeolite film decreased significantly for the dynamic method. The crystals synthesized by the static method and the dynamic method at 165 °C were about 0.9 μm long.

To prepare a continuous film the crystallization temperature was increased to 170 °C. As shown in Fig. 2(d) the crystal size increased to about 1.1 μm and a nearly continuous film was synthesized by the static method. Unfortunately, more crystals were observed in the second layer. It should be noted that continuous zeolite films were observed (Fig. 2(e) and (f)) when the autoclave was rotated at 10 and 20 r/min at 170 °C. Moreover, the number of crystals in the second layer decreased and the film was smoother for the dynamic method compared to the static method.

At the crystallization temperature of 175 °C, the crystal size increased to about 1.2 μm and a continuous zeolite film formed when using the static method (Fig. 2(g)). However, many crystals were observed in the second layer. For the dynamic method, continuous films were observed and the morphologies of the films were smoother (Fig. 2(h) and (i)). The rotation most likely prevented the formation of a second layer on the dense layer.

In our earlier reports [16,17,25], we synthesized continuous films at 165 °C using the static method. The difference in film continuity between our earlier reports and this work is mainly attributed to the amount of synthesis solution. The synthesis solution (20 g) was not more than one-third of the autoclave's volume in the earlier reports while it was more than two-thirds in this work. Longer times were needed for the synthesis solution to reach the set temperature during crystallization in this work.

To confirm the orientation of the zeolite films XRD was carried out, as shown in Fig. 3. Apart from the peak at 2θ = 43.46° that corresponds to the stainless steel substrate, five sharp peaks were observed at 2θ = 8.87°, 17.77°, 26.80°, 35.99°, and 45.45° and these are attributed to the (020), (040), (060), (080), and (0100) orientations of the MFI zeolite crystals [26], respectively. The MFI zeolite films synthesized in our work are predominantly *b*-oriented. However, the two small peaks at 2θ = 35.75° and 45.15°, as shown in Fig. 3(1), are assigned to the (800) and (1000) orientations in the MFI zeolite crystals [26], respectively. The two small peaks indicate that some *a*-oriented MFI crystals were present in the film synthesized using the static method. The amplified drawings show three small peaks that are attributed to the (200), (400), and (600) orientations (data not shown) and these are distinguished with difficulty because of the small peak areas, the overlapping (0k0) peaks and the small difference in 2θ between (h00) and (0k0). Compared with Fig. 3(1), the two peaks attributed to the (800) and (1000) orientations in the MFI zeolite crystals were smaller, as shown in Fig. 3(2), which indicates that less *a*-oriented MFI crystals are present in the film synthesized using the dynamic method. The XRD data (Fig. 3) and the SEM images (Fig. 2) of the films synthesized using the two methods indicate that a better orientation is obtained by dynamic hydrothermal synthesis.

Since the synthesis conditions differed greatly between the static and dynamic hydrothermal methods the size distribution of the zeolite crystals might be different. Figure 4 shows SEM images of the crystal grains grown in the bulk solution at different rotation speeds. Obviously, a large distribution of crystal size was found for the static method. Particle sizes varied from 0.6 to 1.1 μm at R = 0 r/min, as shown in Fig.

4(a). On the contrary, a uniform particle size was found in the bulk solution for the dynamic method (Fig. 4(b) and (c)). This can be attributed to the rotation of the autoclave. In a static environment, apart from settling caused by gravity, quick nutrition consumption around the zeolite crystals resulted in a large concentration gradient. Moreover, a large thermal gradient exists if the stirring is ineffective. In contrast, as effective heat and mass transport is realized by rotation of the autoclave, smaller thermal and concentration gradients exist in the bulk solution for the dynamic method, and this is useful in obtaining MFI particles with a uniform size.

To investigate zeolite film growth the crystallization time was changed from 80 to 120 min. Figure 5 shows SEM images of the zeolite films that formed at 170 °C using different reaction time. Because the static hydrothermal method was used no crystals were observed on the substrate after 80 min (Fig. 5(a)) and only a few disk-shaped crystals were found on the substrate at 90 min (Fig. 5(b)). The disk-shaped crystals grew and were in contact when the crystallization time was increased to 100 and 110 min (Fig. 5(c) and (d)). A nearly continuous film with several pinholes was obtained and some crystals were observed in the second layer when the crystallization time was increased to 120 min (Fig. 2(d)). A continuous zeolite film formed when the crystallization time was increased to 140 min (data not shown here).

As for the dynamic method, a few submicron (0.3 μm) disk-shaped crystals formed in the early crystallization stage (80 min) (Fig. 5(e)). By increasing the crystallization time to 90 min the crystals grew to 0.5 μm and they started to merge with each other (Fig. 5(f)). As the crystallization time was increased to 100 and 110 min, the crystals grew to 0.6 and 0.95 μm, respectively, and the films were nearly continuous (Fig. 5(g) and (h)). A continuous film consisting of crystals of about 1.1 μm in size formed when the crystallization time was increased to 120 min (Fig. 2(f)).

The differences in the films synthesized using these two methods can be attributed to the rotation of the autoclave. The substrate was placed in the middle of the autoclave and a large thermal gradient was evident when using the static method and, therefore, a longer time was needed for the synthesis solution that was near the substrate to reach the set temperature. Therefore, fewer crystals were present on the substrate when using the static method rather than the dynamic method over the same crystallization time.

Considering the homogeneous nucleation mechanism proposed previously [16,17,27] and based on our above results, a film formation mechanism for the dynamic method is proposed as follows: some invisible nuclei form in the bulk solution during 4 h of stirring at room temperature. More nuclei form and the nuclei grow into submicron crystals (0.3 μm) during the early stage of crystallization (the temperature of the bulk solution is much lower than the set crystallization temperature). Some of the submicron crystals are attracted to the substrate surface by favorable electrostatic and van der Waals interactions. By increasing the crystallization time, more crystals are attracted to the substrate surface and they continue to grow. The crystals then merge and form a continuous film when the crystallization time is extended. For the dynamic method, low concentrations and thermal gradients exist in the bulk solution, which causes the solution temperature to increase quickly and a shorter time is needed for the synthesis of a continuous film.

Since the (010) plane has the largest surface area in the MFI crystals, the most stable configuration for submicron crystal settling onto the substrate surface is a *b*-orientation. However, a few *a*-oriented crystals are still present on the substrate surface when using the static method. In a dynamic environment, most of the *a*-oriented crystals that were attracted to the substrate surface wash away or drop down to the substrate surface (transform to *b*-orientation) with the washing action of the bulk solution because the interaction between the *a*-oriented crystals and the substrate surface is weaker than that between the *b*-oriented crystals and the substrate surface. Therefore, a better orientation and smoother film is obtained when using the dynamic method. Moreover, the removal of the *a*-oriented crystals that were attracted to the substrate surface might result in defect filling, which is beneficial for the synthesis of a continuous film.

In conclusion, a rotating convection oven was used to synthesize *b*-oriented MFI zeolite films using a dynamic method. Compared to static hydrothermal synthesis, the dynamic hydrothermal synthesis has some advantages: (1) a shorter synthesis time is required to obtain a continuous film; (2) the orientation of the MFI zeolite film becomes better and the film becomes smoother; (3) the crystal size is more uniform.

Full-text paper available online at ScienceDirect
http://www.sciencedirect.com/science/journal/18722067